Boundary conditions in finite volume schemes for the solution of shallow-water equations: the non-submerged broad-crested weir

Luca Cozzolino, Luigi Cimorelli, Carmine Covelli, Renata Della Morte and Domenico Pianese

ABSTRACT

The broad-crested weir can be regarded as a zone of rapid variation of the bottom elevation that is short with respect to the characteristic length of the considered domain, and for this reason it can be conceptually modelled as a bed step. In this paper, the solution of the Riemann problem for the shallow-water equations over a bed step is exploited in order to simulate the behaviour of the broad-crested weirs, when these are present at the boundaries of the numerical domain. The issue of the multiplicity of solutions for this special Riemann problem is discussed, and rules are given in order to pick up the congruent solution among the alternatives. Finally, the proposed approach is implemented into a finite volume model for the approximate solution of one-dimensional shallow-water equations. Several numerical tests are carried out in order to demonstrate its possibilities and promising capabilities.

Key words | bed step, boundary conditions, broad-crested weir, multiple solutions, Riemann problem, shallow-water equations

Luca Cozzolino (corresponding author)
Renata Della Morte
Department of Engineering,
University of Naples Parthenope,
Centro Direzionale di Napoli,
Isola C4,
80143 Napoli,
Italy
E-mail: *luca.cozzolino@uniparthenope.it*

Luigi Cimorelli
Carmine Covelli
Domenico Pianese
Department of Civil, Architectural and Environmental Engineering,
University of Naples Federico II,
via Claudio 21,
80125 Napoli,
Italy

INTRODUCTION

The quality of the results supplied by numerical models used for the simulation of flow propagation in rivers, or for the inundation assessment in floodplains, is influenced by many aspects. Among others, it is possible to call to mind a few themes on which researchers and technicians have concentrated their efforts, namely the influence of parameters calibration such as the roughness (Vidal *et al.* 2005), the friction model used (Burguete *et al.* 2007), the characterization of simplified flow propagation models (Cimorelli *et al.* 2014) and their numerical implementation (Cimorelli *et al.* 2013), the modelling of geometric source terms (Castro *et al.* 2007), and the influence of coarseness and structure of the computational meshes (Schubert *et al.* 2008).

In the literature, particular attention has been paid to the implementation of the boundary conditions, because in practical computations the numerical domain is truncated at limits that are fixed by the modeller prior to the computations. The information that the flow could freely exchange with the external physical domain must be supplied through these boundaries, and the effects of incorrect implementations, uncertainties, or lack in the quality of physical representation, can propagate inside the numerical domain. Many efforts have been made in order to model special conditions, such as non-reflective boundary conditions at river estuaries (Hu *et al.* 2000), to take into account the uncertainties introduced by the use of the rating curves as boundary conditions (Pappenberger *et al.* 2006; Domenighetti *et al.* 2013), and to enhance the physical representativeness of boundary conditions in one-dimensional flow propagation models with velocities significantly variable through the cross-section (Costabile & Macchione 2012). Real world applications, such as irrigation canals and sewer systems, are often equipped with measure and control structures, or other types of structures that can interfere with the flow, and recent results have been presented in order to enhance the modelling of internal and external boundary conditions

doi: 10.2166/hydro.2014.100

such as sluice gates (Morales-Hernàndez *et al.* 2013), weirs (Guerra *et al.* 2011) and bridges (Catella & Bechi 2006).

In the present paper, attention is focused on structures such as Venturi flumes, broad-crested weirs, sills and side-weirs, and all those structures that can act during their life as broad-crested weirs. Check-dams and other structures used for the control of the erosion in mountain streams, or used for the protection of areas prone to debris flows (Cozzolino *et al.* 2014a), also belong to this category because they behave as flow control devices before being filled by the blocked sediment. In a similar fashion, in small run-of-river water power plants the fixed diversion barrages can act as weirs during high flow periods. In the literature, the weir boundary condition has been often implemented considering the classical weir discharge formula (Zhao *et al.* 1994), but this approach is rigorous only when the flow upstream is steady and subcritical, while its applicability is lost when the flow is supercritical or it is rapidly varied in space and time in proximity of the weir (Sobey 2001). If the numerical model is required to work in the variable conditions that can be found during transients, including supercritical flow, blocking, impact of bores and flow reversal, a general treatment of the boundary condition is required. The application of such an approach to the finite volume schemes is the main subject of the present work.

Different mathematical models have been proposed for the simulation of the flow in open channel networks. Among others, the one- and two-dimensional shallow-water equations, and the De Saint Venant equations, have been widely used for their ability to take into account not only smoothly varying flow conditions, but also flow discontinuities such as hydraulic jumps, moving bores and the flow propagation over dry beds. In order to restrict attention on the mathematical features that characterize the problem of the weir boundary conditions, we simplify the setting of our discussion, and for this reason the propagation model considered here is the system of the one-dimensional shallow-water equations, written in conservative form

$$\frac{\partial \mathbf{u}}{\partial t} + \frac{\partial \mathbf{f}(\mathbf{u})}{\partial x} = \mathbf{s}_b(\mathbf{u}) + \mathbf{s}_f(\mathbf{u}) \tag{1}$$

In Equation (1), the symbols have the following meaning: $\mathbf{u} = (h\ hu)^T$ and $\mathbf{f}(\mathbf{u}) = (hu\ 0.5gh^2 + hu^2)^T$ are the vectors of the conserved variables and of the corresponding fluxes, respectively, h = water depth, u = vertically averaged water velocity, g = gravity acceleration constant, T = matrix transpose, $\mathbf{s}_b(\mathbf{u}) = (0 - gh\mathrm{d}z/\mathrm{d}x)^T$ and $\mathbf{s}_f(\mathbf{u}) = (0 - ghS_f)^T$ are the vectors of the geometric and friction source terms, respectively, z = bed elevation, S_f = friction slope, x = longitudinal coordinate, t = time. The one-dimensional shallow-water equations are established under the hypothesis of rectangular cross-sections with unitary width, and friction confined to the channel bed: despite these restrictive assumptions, the shallow-water equations retain the mathematical structure of the De Saint Venant equations (existence of two families of characteristics, structure of the signal speeds), and for this reason they are well suited for the study of the weir boundary condition without loss of generality. Moreover, a procedure for the treatment of the boundary conditions developed in the setting of the one-dimensional shallow-water equations can be extended easily to the case of the two-dimensional shallow-water equations, exploiting the property of 'rotational invariance' of the two-dimensional shallow-water equations (Toro 2001; Kutija & Murray 2007).

The theoretical equation of the broad-crested weir (Figure 1) can be obtained from the one-dimensional shallow-water equations. First, we observe that if the flow is steady, and the friction is negligible, a solution of Equation (1) can be found after a space-integration between two generic cross-sections 1 and 2 where the flow is gradually varying, obtaining

$$q(h_1, u_1) = q(h_2, u_2), \quad H(h_1, u_1, z_1) = H(h_2, u_2, z_2) \tag{2}$$

In Equation (2), $q(h, u) = hu$ is the specific discharge, $H(h, u, z) = h + u^2/(2g) + z$ is the total head, and the

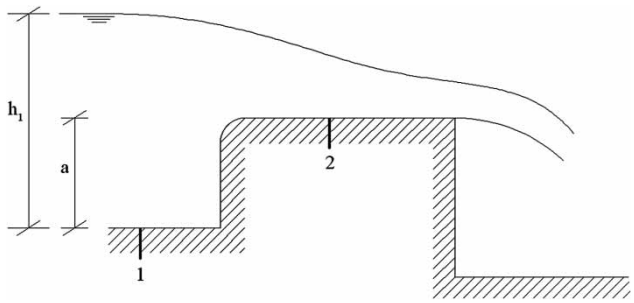

Figure 1 | Broad-crested weir scheme.

subscripts 1 and 2 refer to the corresponding cross-sections. In order to find the weir equation, cross-section 1 is taken immediately upstream of the weir, while cross-section 2 corresponds to the crest of the weir. We make the additional assumptions that the flow is subcritical at cross-section 1, and that the tailwater submergence is below the modular limit (Working Group on Small Hydraulic Structures 1989), implying that the critical flow conditions are attained at the crest (Bélanger's principle). In this case, if $a = z_2 - z_1$ is the height of the weir, we can define the velocity function (Appendix A.1 in Cozzolino *et al.* 2014b).

$$f(a, h_1) = C_d(a, h_1)\sqrt{2gh_1} \tag{3}$$

where

$$C_d(a, h_1) = 2\left(\cos\frac{4\pi + \vartheta}{3}\right)^{\frac{3}{2}},$$
$$\vartheta = \pi + \arctan\left(-\sqrt{\frac{1}{(1 - a/h_1)^2} - 1}\right) \tag{4}$$

The velocity function of Equation (3) must be interpreted as the flow velocity immediately upstream of the broad-crested weir in steady subcritical conditions, and it can be used to obtain the following form of the classic weir equation

$$q = h_1 f(a, h_1) = h_1 C_d(a, h_1)\sqrt{2gh_1} \tag{5}$$

In the technical literature, Equation (5) is usually formulated relating the discharge to the water depth calculated with respect to the weir crest, while the formulation chosen relates the discharge to the water depth h_1 immediately upstream of the structure. This will come to hand when the subsequent mathematical developments are considered.

Many numerical schemes for the solution of the shallow-water equations, such as the finite volume method, the spectral volume method, and the Runge–Kutta discontinuous Galerkin, are based on the use of approximate or exact Riemann solvers for the computation of numerical fluxes at the interfaces between the computational cells. In these models the boundary conditions are usually imposed by means of appropriate values of the numerical fluxes through the domain boundary interfaces. This approach has been widely used in the field of shallow-water equations calculations for the imposition of boundary conditions such as solid walls, inflows and outflows in sub- and supercritical conditions (Zhao *et al.* 1994; Toro 2001), and also weirs (Guerra *et al.* 2011).

The broad-crested weir, and other control structures, can be regarded as bed transitions where the flow characteristics and the bed elevation have a rapid variation over a length of metres. Conversely, the characteristic length of flow propagation problems is of the order of hundreds of metres, or kilometres, and for this reason all these control structures could be conceptually modelled in shallow-water type models as a bed step. Recently, the solution of the shallow-water equations with a bed step has gained great attention (Cozzolino *et al.* 2011), and now general procedures for the analytical solution of the Riemann problem at the frictionless bed step are available for generic flow conditions (Alcrudo & Benkhaldoun 2001; LeFloch & Thanh 2011; Han & Warnecke 2012).

Despite the fact that sudden variations of the flow characteristics are commonly associated with the conservation of momentum (Toro 2001), the energy conservation at bed steps seems appropriate in many cases (Mynett 1999), as proven by the classical treatment of the weir theory. In Cozzolino *et al.* (2014b), the Riemann problem for the shallow-water equations with a frictionless bed step is considered, assuming a dry bed state on the bed step. For this special problem, it is shown that multiple solutions are possible for given initial conditions, and that the multiplicity of the solutions does not depend exclusively on the multiplicity of the possible choices of the path, defining the weak solution in the context of the theory by Dal Maso *et al.* (1995). In the same paper, the idea of using the solution of this Riemann problem as a building block for the construction of appropriate weir boundary conditions is suggested, but the problem of the solutions' multiplicity is not solved. In Guerra *et al.* (2011), a very similar approach for the treatment of the submerged and non-submerged weir boundary conditions is followed, but the case of supercritical flow passing over the crest is not taken into account, and consequently, the issue of multiple solutions is omitted.

Starting from these considerations, in the present paper the analytical solution of the Riemann problem for the shallow-water equations over a dry bed step is exploited in order to simulate the behaviour of the non-submerged broad-crested weir during transients. After having demonstrated that the classical weir equation is a particular solution of this special Riemann problem, it is shown how physical evidence from laboratory experiments available in the literature can be used to pick up the correct solution of the Riemann problem among the alternatives when multiple solutions are possible for given initial conditions. Finally, the proposed approach is implemented into a finite volume model for the approximate solution of the one-dimensional shallow-water equations. Numerical tests are used to demonstrate its performance and its promising capabilities.

THE BED STEP SHALLOW-WATER EQUATIONS

In order to introduce the frictionless sudden bed elevation transitions into shallow-water models, we consider the solution of the bed step shallow-water equations (LeFloch & Thanh 2011)

$$\frac{\partial \mathbf{U}}{\partial t}+\frac{\partial \mathbf{F}(\mathbf{U})}{\partial x}+\mathbf{H}(\mathbf{U})\frac{\partial \mathbf{U}}{\partial x}=0 \tag{6}$$

where the vectors are defined by

$$\mathbf{U}=\begin{pmatrix}\mathbf{u}\\ z\end{pmatrix},\quad \mathbf{F}(\mathbf{U})=\begin{pmatrix}\mathbf{f}(\mathbf{u})\\ 0\end{pmatrix},\quad \mathbf{H}(\mathbf{U})=\begin{pmatrix}0 & 0 & 0\\ 0 & 0 & gh\\ 0 & 0 & 0\end{pmatrix} \tag{7}$$

The system (Equation (6)) cannot be written in conservative form because the non-conservative product $\mathbf{H}(\mathbf{U})\partial\mathbf{U}/\partial x$ is present, and then the classic Rankine–Hugoniot conditions (Toro 2001), which drive moving bores and standing hydraulic jumps in the shallow-water equations, are no longer valid at bed discontinuities. In order to take this difficulty into account, and define the weak solutions for Equation (6), we resort to the theory of Dal Maso *et al.* (1995). If $\mathbf{U}_1$ and $\mathbf{U}_2$ are the states to the left and to the right of a discontinuity, respectively, we assume a path $s\in[0;1]\rightarrow\varphi(s,\mathbf{U}_1,\mathbf{U}_2)$ connecting in the phase space (h, hu, z) the state $\mathbf{U}_1$ to the state $\mathbf{U}_2$, and this path satisfies the following congruency properties: $\varphi(0,\mathbf{U}_1,\mathbf{U}_2)=\mathbf{U}_1$, $\varphi(1,\mathbf{U}_1,\mathbf{U}_2)=\mathbf{U}_2$, $\varphi(s,\mathbf{U},\mathbf{U})=\mathbf{U}\quad\forall s,\mathbf{U}$. When such a path is defined, it is possible to consider the generalized Rankine–Hugoniot conditions $\mathbf{F}(\mathbf{U}_2)-\mathbf{F}(\mathbf{U}_1)-\mathbf{S}_\varphi(\mathbf{U}_1,\mathbf{U}_2)=\xi(\mathbf{U}_2-\mathbf{U}_1)$, where the term

$$\mathbf{S}_\varphi(\mathbf{U}_1,\mathbf{U}_2)=-\int_0^1\mathbf{H}(\varphi(s,\mathbf{U}_1,\mathbf{U}_2))\frac{\partial\varphi}{\partial s}(s,\mathbf{U}_1,\mathbf{U}_2)\,ds \tag{8}$$

takes into account the effect of the non-conservative product $\mathbf{H}(\mathbf{U})\partial\mathbf{U}/\partial x$ through the discontinuities, while ξ is the propagation celerity of the discontinuities. When the bed is smooth, the classic Rankine–Hugoniot conditions $\mathbf{F}(\mathbf{U}_2)-\mathbf{F}(\mathbf{U}_1)=\xi(\mathbf{U}_2-\mathbf{U}_1)$ are recovered because the term $\mathbf{S}_\varphi(\mathbf{U}_1,\mathbf{U}_2)$ is null. We observe that the celerity of the discontinuity is null at bed steps because these are fixed, and then the generalized Rankine–Hugoniot conditions reduce to

$$\mathbf{F}(\mathbf{U}_2)-\mathbf{F}(\mathbf{U}_1)=\mathbf{S}_\varphi(\mathbf{U}_1,\mathbf{U}_2) \tag{9}$$

The analytic solution of the Riemann problem at the dry step

The classical weir equation (Equation (5)) is valid only in the hypothesis of steady flow, with subcritical flow conditions immediately upstream of the structure. Aiming at relaxing these assumptions, and in order to consider a variety of conditions that can be encountered during transients, we consider a Riemann problem where Equation (6) is solved considering the following initial conditions

$$\mathbf{U}(x,0)=\begin{cases}\mathbf{U}_L, & x<0\\ \mathbf{U}_R, & x>0\end{cases},\quad \mathbf{U}_L=(\,h_L\quad h_Lu_L\quad 0\,)^T,\quad \mathbf{U}_R=(\,0\quad 0\quad a\,)^T,\quad a\geq 0 \tag{10}$$

Equations (6) and (10) define a special initial-value problem where the constant states $\mathbf{U}_L$ and $\mathbf{U}_R$ are separated by a discontinuity of the flow variables and of the bottom elevation, and the quantity $a\geq 0$ is interpreted as the height

of the weir. The self-similar solution of the Riemann problem defined by Equations (6) and (10) is characterized by the external states $\mathbf{U}_L$ and $\mathbf{U}_R$, connected by one or more waves that separate one or more intermediate states, and we call $\mathbf{U}_1 = (h_1 \quad h_1u_1 \quad 0)^T$ and $\mathbf{U}_2 = (h_2 \quad h_2u_2 \quad a)^T$ the states immediately to the left and to the right of the bed discontinuity, respectively. In order to define the solution at frictionless bed steps, we can choose from the literature one of the following implicit definitions D1, D2 or D3 for the path linking the states $\mathbf{U}_1$ and $\mathbf{U}_2$.

Definition D1 for the path φ

The energy is conserved along the frictionless bed transition when the discharge through the step is not null (Alcrudo & Benkhaldoun 2001), and then the states $\mathbf{U}_1$ and $\mathbf{U}_2$ are linked by the condition expressed in Equation (2).

Definition D2 for the path φ

There is a bed elevation z_M, intermediate between the elevations z_1 and z_2, where a standing hydraulic jump is collocated (Baines & Whitehead 2003), and the intermediate states $\mathbf{U}_M^- = (h_M^- \; h_M^- u_M^- \; z_M)^T$ and $\mathbf{U}_M^+ = (h_M^+ \quad h_M^+ u_M^+ \quad z_M)^T$ are connected by the hydraulic jump condition $\mathbf{F}(\mathbf{U}_M^-) = \mathbf{F}(\mathbf{U}_M^+)$. The state $\mathbf{U}_1$ is linked to the state $\mathbf{U}_M^-$ by the discharge and head conservation conditions $q(h_1, u_1) = q(h_M^-, u_M^-)$ and $H(h_1, u_1, z_1) = H(h_M^-, u_M^-, z_M^-)$, respectively, while the state $\mathbf{U}_M^+$ is linked to the state $\mathbf{U}_2$ by the conditions $q(h_M^+, u_M^+) = q(h_2, u_2)$ and $H(h_M^+, u_M^+, z_M^+) = H(h_2, u_2, z_2)$, respectively. The state $\mathbf{U}_2$ corresponds to critical flow conditions.

Definition D3 for the path φ

When the discharge is null, the following conditions are taken (Han & Warnecke 2012): $h_1 \le a$, $u_1 = 0$, $h_2 = 0$, $u_2 = 0$.

The general methods described in LeFloch & Thanh (2011), and Han & Warnecke (2012), can be used to solve the Riemann problem of Equations (6) and (10), complemented by the definitions D1, D2 or D3 of the path φ connecting the states at the bed step. In Cozzolino *et al.* (2014b), the cited Riemann problem is solved considering different states $\mathbf{U}_L$, and it is shown that there are initial conditions that admit multiple solutions. In particular, if $F_L = u_L/\sqrt{gh_L}$ is the Froude number related to the state $\mathbf{U}_L$, and a/h_L is the specific height of the bed step, it is possible to draw a classification diagram (see Figure 2) inspired by that presented in Mehrotra (1974), where eight different classes of solutions called *regimes* (from R-I to R-VIII) are collocated. The curves of the plane $(a/h_L, F_L)$ separating the fields of existence of the regimes are described by the equations contained in Table 1, and from Figure 2 it is apparent that these fields of existence may overlap partially. For each regime, the states $\mathbf{U}_1$ and $\mathbf{U}_2$ can be calculated using the analytical approach summarized in Table 2, where the path definitions used are also reported, together with a brief description of the regime itself.

The numerical broad-crested weir boundary condition

When the definition D1 for the path φ is used, the assumptions made in order to establish the solution of the bed step Riemann problem (discharge and head conservation through the bed transition) are the same made in order to establish the broad-crested weir boundary condition. In this sense, the solution of the bed step Riemann problem can be considered a generalization of the broad-crested weir behaviour to general transients. In order to confirm this, we have only to show that the solution of the Riemann problem defined by Equations (6) and (10) is congruent with the weir boundary condition when the flow is stationary. Aiming at this, we observe that if h_L and u_L are linked by Equation (3), the flow conditions corresponding to the

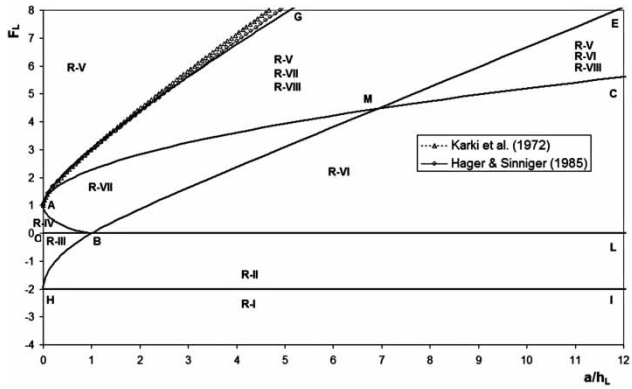

Figure 2 | Riemann problem for the broad-crested weir: fields of existence of the solutions.

Table 1 | Curves limiting the fields of validity of the regimes in the (a/h_L, F_L) plane

Curve	Definition
AG	$1+\frac{F_L^2}{2}-\frac{3}{2}\sqrt[3]{F_L^2}-\left(\sqrt{1+8F_L^2}-3\right)^3\Big/\left[16\left(\sqrt{1+8F_L^2}-1\right)\right]-\frac{a}{h_L}=0.$
BAMC	$1+\frac{F_L^2}{2}-\frac{3}{2}\sqrt[3]{F_L^2}-\frac{a}{h_L}=0.$
BME	$F_L-\left(\frac{a}{h_L}-1\right)\sqrt{\frac{1}{2}\left(1+\frac{h_L}{a}\right)}=0.$
HB	$\left(1+\frac{F_L}{2}\right)^2-\frac{a}{h_L}=0.$
OBL	$F_L=0.$
HI	$F_L+2=0.$

Table 2 | Analytical solution of the Riemann problem at the dry step

Regime	Path definition	Analytic solution	Brief description
R-I	D3	$h_1=0,\ u_1=0,\ h_2=0,\ u_2=0.$	$F_L\le -2$ and then there is cavitation at the bed step.
R-II	D3	$h_1=h_L\left(1+\frac{F_L}{2}\right)^2,\ \ u_1=0,\ \ h_2=0,\ \ u_2=0.$	The flow with $-2<F_L<0$ is blocked.
R-III (1)	D1	Find h_1 and u_1 solving the system $\begin{cases} u_L+2\sqrt{gh_L}=u_1+2\sqrt{gh_1} \\ u_1=f(a,h_1) \end{cases}$. Calculate $h_2=\sqrt[3]{(h_1u_1)^2/g},\quad u_2=h_1u_1/h_2.$	The flow with $-2<F_L<0$ passes over the step.
R-IV	D1	The same as for regime R-III.	The flow with $0\le F_L<1$ moves with head greater than that strictly sufficient to pass over the step.
R-V	D1	$h_1=h_L,\ u_1=u_L.$ Find h_2 selecting the supercritical flow solution of $H(\mathbf{U}_2)=H(\mathbf{U}_L)$. Calculate $u_2=h_1u_1/h_2.$	The flow with $F_L\ge 1$ moves with head greater than that strictly sufficient to pass over the step.
R-VI	D3	$u_1=0,\ h_2=0,\ u_2=0.$ Find h_1 solving $u_L=(h_1-h_L)\sqrt{\frac{g}{2}\frac{h_1+h_L}{h_1h_L}}$.	The flow with $F_L\ge 0$ is blocked.
R-VII (1)	D1	Find h_1 and u_1 solving the system $\begin{cases} u_1=u_L-(h_1-h_L)\sqrt{\frac{g}{2}\frac{h_1+h_L}{h_1h_L}} \\ u_1=f(a,h_1) \end{cases}$. Calculate $h_2=\sqrt[3]{(h_1u_1)^2/g},\quad u_2=h_1u_1/h_2.$	The flow with $F_L>0$ moves with head minor than that strictly sufficient to pass over the step.
R-VIII	D2	$h_1=h_L,\ u_1=u_L.$ Calculate $h_2=\sqrt[3]{(h_1u_1)^2/g},\quad u_2=h_1u_1/h_2.$	The flow with $F_L\ge 1$ produces a hydraulic jump along the bed transition.

(1): The function $f(a, h_1)$ is defined by Equation (3).

state $\mathbf{U}_L$ are those found immediately upstream of the weir in subcritical stationary conditions. In this case, the point (F_L, a/h_L) lies on the arc AB of the curve BAMC in Figure 2, and the arc AB is the boundary between the fields of existence of the regimes R-IV and R-VII. From an inspection of Table 2 it is clear that both regimes R-IV and R-VII supply $h_1 = h_L$ and $u_1 = u_L$ for $u_L = f(a, h_L)$, and then no propagating wave connects the state $\mathbf{U}_L$ to the state $\mathbf{U}_1$ because $\mathbf{U}_1 = \mathbf{U}_L$. This shows that the flow field upstream of the weir does not start to evolve, and that the stationary conditions upstream of the weir are kept indefinitely. In conclusion, if the flow $\mathbf{U}_L$ upstream of the weir is subcritical and stationary, and it satisfies the weir boundary condition, the solution of the Riemann problem does not alter this equilibrium.

Having demonstrated that the theoretical weir equation is a special solution of the Riemann problem considered, we now consider the issue of the multiplicity of solutions for a given state $\mathbf{U}_L$. Inspection of Figure 2 shows that the field EGAM admits the regimes R-V, R-VII and R-VIII, while the field CME admits the regimes R-V, R-VI and R-VIII. The multiplicity of solutions is not only a consequence of the multiplicity of choices of the path's definition, because the regimes R-V and R-VII, based on the definition D1, superpose in the field EGAM. This observation seems to make the analytical solutions presented in Cozzolino *et al.* (2014b) useless for the establishment of a broad-crested weir boundary condition valid for general conditions and during transients.

In order to discuss how we can disambiguate the problem, choosing properly one solution among the alternatives, we make first some observations on the meaning of the mathematical representation of bed steps. The shallow-water equations admit solutions containing discontinuities, and these zero-length discontinuities are intended to represent those phenomena (standing hydraulic jumps, moving bores) where the velocity and depth vary rapidly over a finite length. The length where these real fluid phenomena develop (metres) is often small with respect to the characteristic length of the problem at hand (hundreds of metres or kilometres), making the mathematical discontinuity a numerically accurate representation of the physical phenomena. In a similar fashion, bed discontinuities can be used not only to represent abrupt steps, but can be used also to model smooth transitions of the bed where the elevation varies significantly on a short length (Ostapenko 2002). For this reason, steps at the end of stilling basin aprons, broad-crested weirs, inlet and outlet transitions of Venturi flumes, sills, and other structures, could all be represented by a bed elevation discontinuity. The substitution of a finite-length structure with a bed step reduces the computational burden because the use of very fine numerical grids for the representation of rapid bottom variations is avoided, and this is convenient. Nonetheless, the savings made in terms of computational effort do not come for free, and it is possible that the given initial value problem admits multiple solutions. This ambiguity arises after the cancellation of the actual bed profile, which is substituted by the bed step. In this sense, the bottom step approximation conserves the memory of the different solutions corresponding to the original bed profiles, but the ability to discriminate among these solutions is lost. This implies that, when multiple solutions of the Riemann problem of Equations (6) and (10) are available, the choice of one solution from the set of alternatives should be made by the modeller using the knowledge about the physics of the phenomenon that is external to the mathematical model, and taking into account the actual profile of the channel bottom which is modelled by means of a step. For the case of the broad-crested weir, we observe what follows.

Exclusion of regime R-VIII

Due to the sub-vertical profile of the broad-crested weir, the actual length of the bed discontinuity is null, while the length of the hydraulic jump is always finite. This implies that the solutions that allow the existence of a hydraulic jump entirely contained along the upstream face of the structure (path definition D2) are excluded, and then regime R-VIII is never appropriate in the present situation.

Regime R-VI prevails over R-V

The sub-vertical profile of the broad-crested weir forces strong vertical components of the flow immediately upstream of the weir. For this reason, a structure with height a greater than a limit defined by the arc BME in Figure 2 acts as a wall, and the flow is blocked. This implies that when both regimes R-V and R-VI are solutions of the

Riemann problem, regime R-VI is chosen and regime R-V is excluded.

Regime R-VII prevails over R-V

The laboratory experiments conducted by Karki *et al.* (1972), approximately characterized by $F_L \in [1.5; 3.7]$ and $a/h_L \in [0.25; 1.25]$, show that there are values of F_L and a/h_L such that the supercritical flow impinging on a non-ventilated sill with vertical upstream face is able to pass over the structure without becoming subcritical. In particular, Karki *et al.* (1972) present a criterion (represented in Figure 2 with triangles) in order to discriminate between this situation (regime R-V) and the condition where the supercritical flow becomes subcritical before passing over the sill (regime R-VII). Hager & Sinniger (1985) discuss a number of laboratory experiments from the literature, approximately characterized by $F_L \in [1.5; 10]$ and $a/h_L \in [0.20; 6.5]$, confirming that there are conditions where a supercritical flow is able to pass over the step without causing the formation of a hydraulic jump. When the bed step is vertical, no 'hydraulic hysteresis' effect (Mehrotra 1974) is found, the passage from one condition to the other is abrupt, and the two conditions are always mutually exclusive for a given couple of values (F_L, a/h_L). A limit criterion is suggested also by these authors, and it is represented in Figure 2 with circles. Both the limit criteria from the literature, confirmed by the physical experiments, are very close for $F_L < 6$ to the theoretical curve AG that separates the field of validity of the regime R-V from the field where both regimes R-V and R-VII are possible. We conclude saying that, in order to be congruent with the physical evidence, regime R-VII must prevail over regime R-V in the field where both solutions are possible, if the upstream face of the bed step is vertical.

DESCRIPTION OF THE NUMERICAL MODEL

The analytical solution of the Riemann problem for the broad-crested weir is implemented as a boundary condition option into the first-order finite volume scheme for the approximate solution of the shallow-water equations, derived from the third-order spectral volume model described in Cozzolino *et al.* (2012). The one-dimensional physical domain is partitioned into NV non-overlapping control volumes, and the shallow-water equations are integrated in each control volume, obtaining the following set of ordinary differential equations:

$$\frac{d\mathbf{u}_i}{dt} = -\frac{1}{\Delta x_i}\left(\mathbf{f}_{i+1/2} - \mathbf{f}_{i-1/2}\right) + \mathbf{s}_{b_i} + \mathbf{s}_{f_i}, \quad i = 1, 2, \ldots, NV \tag{11}$$

where Δx_i is the length of the generic finite volume C_i, $\mathbf{u}_i = \begin{pmatrix} h_i & hu_i \end{pmatrix}^T$ is the vector of the conserved variables averaged over C_i, and $\mathbf{s}_{b_i}$ and $\mathbf{s}_{f_i}$ are suitable numerical approximations of the geometric and friction source terms, respectively. In Equation (11), $\mathbf{f}_{i+1/2} = \mathbf{f}\left(\mathbf{u}^-_{i+1/2}, \mathbf{u}^+_{i+1/2}\right)$ is the vector of numerical fluxes through the interface $i + 1/2$ between the cells C_i and C_{i+1}, while $\mathbf{u}^-_{i+1/2} = \begin{pmatrix} h^-_{i+1/2} & hu^-_{i+1/2} \end{pmatrix}^T$ and $\mathbf{u}^+_{i+1/2} = \begin{pmatrix} h^+_{i+1/2} & hu^+_{i+1/2} \end{pmatrix}^T$ are the vectors of the conserved variables reconstructed to the left and to the right of the same interface following the approach by Audusse *et al.* (2004). A small limit depth ε_h is defined in order to distinguish between dry cells, where the flow velocity is assumed null, and the wet cells, where the momentum equation is adjourned as ordinary. The numerical fluxes are evaluated using the HLLE approximate Riemann solver (Einfeldt 1988), while the geometric source terms $\mathbf{s}_{b_i} = \mathbf{s}^+_{b_{i-1/2}} + \mathbf{s}^-_{b_{i+1/2}}$ is defined as the sum of the interface contributions $\mathbf{s}^+_{b_{i-1/2}}$ and $\mathbf{s}^-_{b_{i+1/2}}$, and is calculated following the approach by Audusse *et al.* (2004). While the hyperbolic part of Equation (11) is solved by means of the explicit Euler algorithm, the implicit Euler step is used in order to evaluate the friction terms.

Implementation of the broad-crested weir boundary condition

In order to show how the solution of the broad-crested weir Riemann problem can be used to impose the weir boundary condition, we hypothesize that a broad-crested weir with height a is present at the right boundary of the one-dimensional domain. In this case, $\mathbf{U}_L$ coincides with the state in the right end control volume of the numerical domain, and we make the positions $h_L = h_{NV}$ and $u_L = hu_{NV}/h_{NV}$. After the calculation of the quantities F_L and a/h_L, the corresponding regime for the Riemann problem of Equations

(6) and (10) is individuated from the classification diagram (Figure 2), and this allows the calculation of the states $\mathbf{U}_1$ and $\mathbf{U}_2$ immediately to the left and to the right of the bed discontinuity, respectively, using the analytical approaches reported in Table 2. When multiple solutions are possible, the disambiguation criteria contained in the preceding section are used.

Once $\mathbf{U}_1$ and $\mathbf{U}_2$ are known, we derive from Equation (9) the following numerical flux and geometric source term that are imposed at the end interface of the numerical domain in Equation (11):

$$\mathbf{f}_{NV+1/2} = \begin{pmatrix} h_2 u_2 & \frac{1}{2} g h_2^2 + h_2 u_2^2 \end{pmatrix}^T, \quad \mathbf{s}^-_{b_{NV+1/2}} = \begin{pmatrix} 0 & \frac{1}{2} g h_2^2 + h_2 u_2^2 - \frac{1}{2} g h_1^2 - h_1 u_1^2 \end{pmatrix}^T \tag{12}$$

A naive broad-crested weir boundary condition

Prior to evaluating the numerical method proposed in this section, we describe also a naive implementation of the weir boundary condition, based on the direct imposition of the discharge formula of Equation (5). For this naive procedure, the positions $h_L = h_{NV}$ and $u_L = hu_{NV}/h_{NV}$ are made immediately upstream of the bed step. If $h_L \le a$, an exact wall boundary condition is used, and then h_1 is calculated assuming the regime R-I if $F_L < -2$, the regime R-II if $-2 \le F_L < 0$, and the regime R-VI if $F_L \ge 0$, while $u_1 = u_2 = h_2 = 0$. If $h_L > a$, then $h_1 = h_L$ and $u_1 = u_L$, while the specific discharge q over the weir is calculated by means of Equation (5). Once q is known, the flow characteristics over the weir are found hypothesizing critical state conditions, and then $h_2 = \sqrt[3]{(h_1 u_1)^2/g}$ and $u_2 = h_1 u_1 / h_2$ are calculated. With these definitions of the states $\mathbf{U}_1$ and $\mathbf{U}_2$, the numerical flux and the geometric source term at the boundary are calculated using Equation (12).

In summary, during the generic transient the naive boundary condition approximates the solution of the Riemann problem of Equations (6) and (10) by means of the solution valid for steady subcritical flow. This procedure is expected to supply accurate results when the state $\mathbf{U}_L$ lies close to the arc AB of Figure 2, that is, when the quantity $|u_L - f(a, h_L)|$ is small.

NUMERICAL EXPERIMENTS

In this section, the numerical method proposed is used to reproduce the results of a laboratory experiment characterized by highly variable conditions, in order to verify its applicability to realistic applications. Other simplified tests are used to highlight the differences between the procedure proposed and the naive algorithm described in the preceding section.

CADAM test

The results of the numerical model are compared with the experimental data of a laboratory dam-break (Hiver 2000). The original experimental set-up consisted of a $L = 38$ m long horizontal channel, with rectangular cross-section of constant width $B = 0.75$ m, in which a gate separated a 15.5 m long reservoir from the downstream portion of the channel. A symmetric triangle-shaped sill, 6 m long and 0.40 m high, was located 10 m downstream of the gate, and the Manning coefficient $n = 0.0125$ s m$^{-1/3}$ was evaluated for the channel bed. At the upstream end of the channel, the boundary condition consisted of a wall, while at the downstream end of the channel a weir with height $a = 0.15$ m was located. The initial conditions were characterized by a reservoir filled with $h_u = 0.75$ m of water, and a pool filled with $h_d = 0.15$ m of water between the bump and the downstream weir (see Figure 3): the sudden removal of the gate allowed reproduction of the instantaneous failure of a dam and the flooding of the pool downstream. Nine

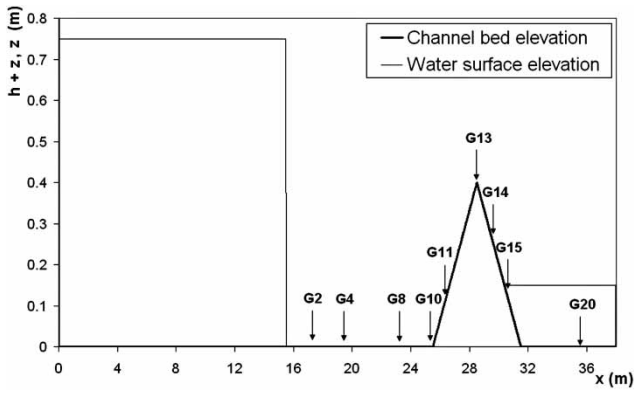

Figure 3 | Laboratory dam-break experiment: gauges' position and initial conditions.

gauges (G2, G4, G8, G10, G11, G13, G14, G15, G20) were installed at different distances from the gate (see Table 3), in order to measure the water depth variations during the transient caused by the dam failure: in particular, gauges from G2 to G11 were collocated to the left of the triangular sill top, while the gauge G13 was collocated at the sill top, and the gauges from G14 to G20 were collocated to the right (Figure 3). After the gate removal at $t = 0$ s, the toe of the dam-break profile reached the sill at about $t = 3$ s, overtopped it at time $t = 4$ s, and then invaded the pool to the right, causing the formation of waves in the pool and the loss of water through the end weir. In order to numerically reproduce this test, the computational domain is subdivided into $NV = 760$ uniform finite volumes ($\Delta x = 0.05$ m), with time step $\Delta t = 0.025$ s and limit depth $\varepsilon_h = 10^{-7}$ m, while the friction slope is calculated using the Manning formula with roughness coefficient $n = 0.0125$ s m$^{-1/3}$.

Aiming at the evaluation of the procedure proposed for the treatment of the weir boundary condition, we determine if there is a control volume of the experimental apparatus where the flow is influenced exclusively by the presence of the weir at the channel end, at least during well-defined time intervals. In Figure 4, the numerical and the laboratory experiment results are compared for the gauges from G14 to G20. At G14, which is immediately downstream of the sill top, the water height is consistently underpredicted: this shows that the shallow-water equations cannot take into account all the real water effects, such as turbulence, flow separation and mixing with air, which can dominate the flow immediately downstream of obstacles and topographies with high curvature. Nonetheless, a closer inspection of the laboratory and numerical results at G14 shows that it is possible to individuate two time intervals ($t \in [25; 40]$ and $t \in [52; 72]$) characterized by zero depth, and this guarantees the separation between the flows to the left and to the right of the triangular sill, during the same intervals.

The gauges G15 and G20 are collocated in the pool at a short distance from the end weir, and are characterized by complicated water depth patterns, due to the interaction between the waves overtopping the triangular sill and the

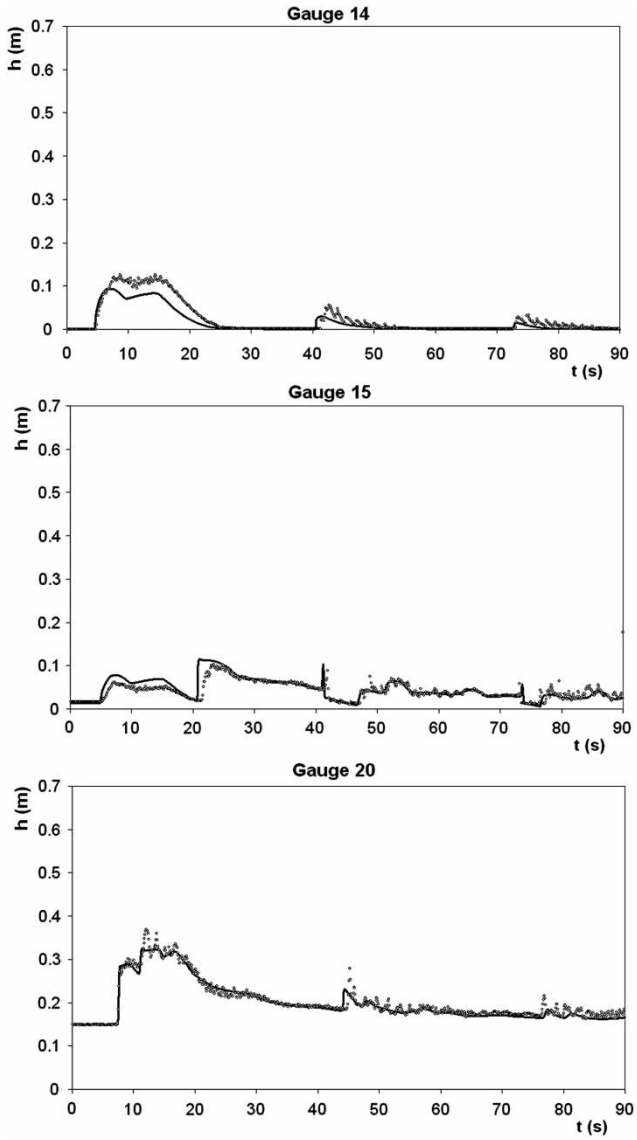

Figure 4 | Laboratory dam-break experiment: comparison between experimental (circles) and numerical results (continuous line) for gauges G14, G15 and G20 (water depth).

Table 3 | Laboratory dam-break experiment: gauge positions

Gauge	Abscissa (m)
G2	17.5
G4	19.5
G8	23.5
G10	25.5
G11	26.5
G13	28.5
G14	29.5
G15	30.5
G20	35.5

waves partially reflected by the weir. Despite these strong interactions, the numerical and the experimental results agree quite well. In particular, recalling the observations made for G14, it is clear that for times $t \in [25; 40]$ and $t \in [52; 72]$ the flow in the pool is governed only by the presence of the weir. For these time intervals, the numerical results follow almost perfectly the experimental results, thus indirectly confirming the applicability of the proposed procedure to the treatment of the weir boundary condition.

In order to appreciate the intrinsic difficulty to implement correctly a boundary condition able to reproduce the weir behaviour during transients, it is instructive to inspect the results supplied for the same study case by other authors (gauge G20 of Figure 14 in Rebollo *et al.* 2003; Figure 12(d) in Zhou *et al.* 2004). The numerical methods proposed in these works underestimate the laboratory results in the zone close to the weir, showing that the implementation of this type of boundary condition is not a trivial task.

The numerical results of the naive procedure are not reproduced here because they behave well for this test case, and are almost indistinguishable from the numerical results supplied by the complete procedure. In order to investigate this circumstance, we consider the flow conditions in the last cell of the numerical domain. In Figure 5, the trajectory of these flow conditions is plotted in the plane $(a/h_L, F_L)$, having set $h_L = h_{NV}$ and $u_L = hu_{NV}/h_{NV}$. The inspection of the figure shows that, during the simulation, the flow conditions in the last cell of the numerical domain lie very close to the arc separating

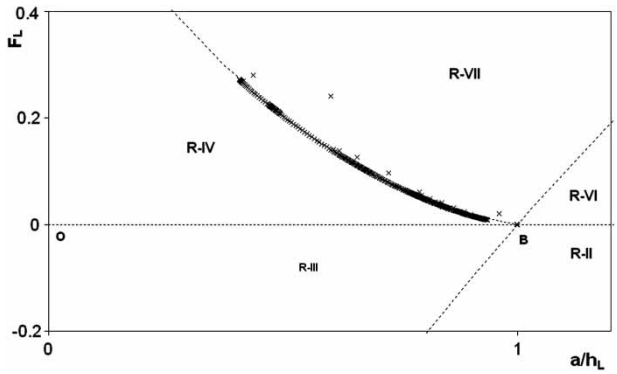

Figure 5 | Laboratory dam-break experiment: the crosses represent the trajectory in the $(a/h_L, F_L)$ plane of the flow conditions immediately upstream of the weir.

regimes R-IV and R-VII, and then very close to the steady subcritical flow conditions implicitly defined by Equation (5). In other words, the flow conditions in the last cell of the domain are in balance with the weir during the simulation. When this happens, the assumptions made to establish the naive boundary conditions are met, and the direct use of Equation (5) supplies accurate results.

In general, the time that the weir takes to influence directly the state $\mathbf{U}_L$ is proportional to the cell length, and tends to zero for grid spacing tending to zero. This implies that the naive boundary condition has the same accuracy of the complete procedure on refined numerical grids, because the state $\mathbf{U}_L$ is always close to a balance with the boundary condition during the entire transient. This condition is actually met in the present test case, because the state $\mathbf{U}_L$ used for the application of the boundary condition procedures refers to a control volume whose centre is at only 0.025 m from the downstream end of the channel. Conversely, the time needed to drive the state $\mathbf{U}_L$ towards a balance with the boundary condition is large for coarse grids, and the assumptions made to establish the naive boundary conditions are inconsistent in this case. On coarse grids, the complete procedure behaves better because it solves accurately the Riemann problem at the boundary also for states $\mathbf{U}_L$ that are not close to the arc AB of Figure 2. This will be apparent in the following numerical tests.

Supercritical flows over a sill

The proposed numerical method is tested with reference to the passage of a supercritical flow over a sill where the energy is conserved. This condition is not a mere mathematical curiosity, even for very high Froude numbers, being instead a phenomenon to be considered in many circumstances. For example, stilling basins are structures where the energy dissipation of supercritical flows can be obtained by forcing the formation of a hydraulic jump, and the containment of the hydraulic jump roller into the basin is ensured using a downstream sill. The formation of a supercritical flow able to jump over the sill is a condition to be avoided (Hager & Sinniger 1985). Of course, flow with high Froude numbers are found in many other conditions, and it is possible to consider natural and man-originated phenomena such as the impact of dam-break waves and debris flows on

obstacles, sills and other control structures, and the propagation of flood waves in mountain streams as well.

In this numerical experiment, we consider a channel $L = 10$ m long, without friction, where a broad-crested weir with height $a = 0.50$ m is present at the right boundary, while the left boundary is open. The initial conditions are characterized by $h(x,\ 0) = 0.45\,\text{m}$ and $u(x,\ 0) = 8.50\,\text{m/s}$, and the same values of the depth and velocity are imposed at the left end. This condition corresponds to the regime R-V, and then the flow is expected to remain supercritical through the end sill. In order to perform this numerical test, the computational domain is subdivided into $NV = 20$ uniform finite volumes ($\Delta x = 0.50$ m), and the time step $\Delta t = 0.02$ s is used. In Figure 6, the analytic solution of this problem is compared with the numeric solution (open circles) at time $t = 10.0$ s, with reference to the water depth h (left panel). Eye inspection of the figure shows that the analytical and the numerical solutions are almost indistinguishable, and this is confirmed by a close inspection of the numerical results tabulated at the end of the calculations. Actually, the procedure proposed in this paper is capable, by construction, to discriminate the actual flow conditions over the weir, also in supercritical flow conditions.

In the same panel, the results obtained by the naive scheme are represented with crosses. The inspection of the figure shows that the naive treatment introduces a flow depth error at the right end of the channel, where the flow is forced to become subcritical. The superficial observation that the errors are confined to a limited portion of the computational domain could support a general use of the naive procedure, also in supercritical conditions. In fact, this conclusion is illusory, because the bad representation of the flow depth at the end of the channel induces an unacceptable error: if the water depth at the end of the channel is used to evaluate the specific discharge flowing over the weir by means of Equation (5), the value $q = 4.077\ \text{m}^2/\text{s}$ is obtained, which is in contrast with the analytical solution $q = 3.825\ \text{m}^2/\text{s}$, and the mass conservation is violated. Of course, this error is not eliminated if the grid is refined, because the naive boundary treatment is not able to take into account the case of supercritical flow upstream of the weir. This counterexample demonstrates that a general treatment for the weir boundary conditions is required, in order to correct the issues introduced by simplified approaches.

Another example is considered, with initial conditions $h(x,\ 0) = 1.00\,\text{m}$ and $u(x,\ 0) = 4.70\,\text{m/s}$, and the same values of the depth and velocity are imposed upstream, while $a = 0.80$ m. This time, the flow conditions correspond to regime R-VII (with $F_L > 1$), and then the supercritical flow becomes subcritical through a hydraulic jump that moves backwards. A coarse grid is considered in order to perform this numerical test, and the computational domain is subdivided into $NV = 20$ uniform finite volumes ($\Delta x = 0.50$ m), while the time step $\Delta t = 0.01$ s is used. In Figure 6 (right panel), the analytical solution of this problem is compared with the numerical solution (open circles) at time $t = 3.0$ s, with reference to the water depth h. Despite the numerical dissipation that smooths the flow depth profile, the procedure based on the analytical solution of the bed step Riemann problem captures with fidelity the position of the moving discontinuity, together with the flow depth at the weir. In the same panel, the results supplied by the naive boundary conditions are also presented for the same coarse grid, and it is interesting to observe that

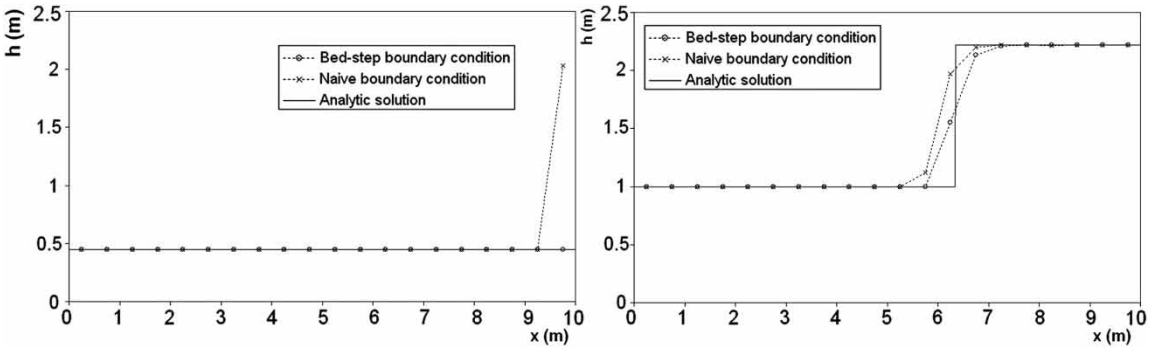

Figure 6 | Supercritical flow over a sill: regime R-V (left panel) and regime R-VII (right panel).

the naive procedure misses the hydraulic jump position, while this error can be eliminated if the grid is refined. The naive and the complete procedures converge to the same solution when subcritical flow conditions are expected upstream of the weir, but the complete procedure supplies more accurate results on coarse grids.

Cavitation at the bed step

Cavitation numerical experiments are commonly used to evaluate the robustness of numerical methods with respect to the formation of dry bed (Toro 2001). A channel $L = 10$ m long is considered, without friction, where a broad-crested weir $a = 0.20$ m high is present at the right boundary, while the left boundary is open. The initial conditions are characterized by $h(x,\ 0) = 1.00\,\text{m}$ and $u(x,\ 0) = -6.30\,\text{m/s}$, and the same values of the depth and velocity are imposed at the left end. This condition corresponds to the regime R-I, and then the cavitation of the flow is expected at the toe of the broad-crested weir. In order to perform this numerical test, the computational domain is subdivided into $NV = 20$ uniform finite volumes ($\Delta x = 0.50$ m), and the time step $\Delta t = 0.025$ s is used. In Figure 7, the analytical solution of this problem is compared with the numerical solution (open circles) at time $t = 0.2$ s, with reference to the water depth h. Despite the coarse numerical grid used, the numerical procedure based on the analytical solution of a bed step Riemann problem seems to capture the main features of the problem, namely the strength of the rarefaction and its position, while the discharge through the end weir is null as expected.

In the same figure, the results supplied using the naive boundary condition are represented. It is seen that a spurious wave appears in the naive solution. In fact, the naive boundary condition supplies a discharge greater than zero through the weir at the beginning of the transient, and this in turn causes the overestimation of the thrust exerted by the weir on the flow, with a consequent acceleration of the flow. Also in this case, the spurious wave introduced by the naive treatment of the boundary condition disappears if the grid is refined and very short time steps are used.

Subcritical flow chocked at the bed step

In the present test case, we consider a subcritical flow with energy insufficient to pass over the broad-crested weir, and for this reason it is chocked by a bore that moves upstream while critical conditions are attained at the weir crest (regime R-VII with $F_L < 1$). In a channel $L = 10$ m long, without friction, where a broad-crested weir $a = 0.50$ m high is present at the right boundary, and the left boundary is open, the initial conditions are characterized by $h(x,\ 0) = 1.00\,\text{m}$ and $u(x,\ 0) = 1.50\,\text{m/s}$, and the same values of the depth and velocity are imposed at the left end. In order to perform this numerical test, the computational domain is subdivided into $NV = 20$ uniform finite volumes ($\Delta x = 0.50$ m), and the time step $\Delta t = 0.05$ s is used. In Figure 8, the analytical solution of this problem is compared with the numerical solution (open circles) at time $t = 0.5$ s, with reference to the water depth h. Inspection of the figure shows that the numerical dissipation smooths the numerical

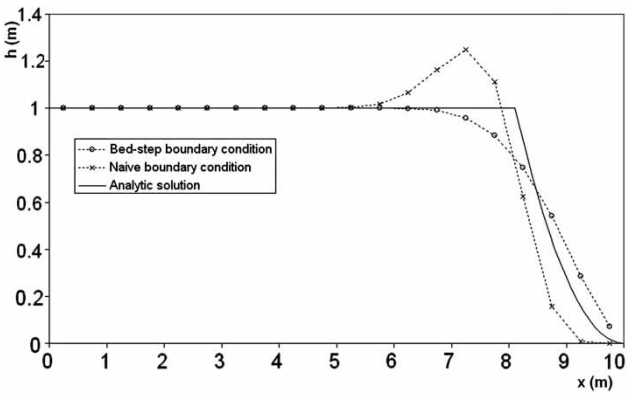

Figure 7 | Cavitation at the weir: comparison between the analytical solution and the numerical experiments.

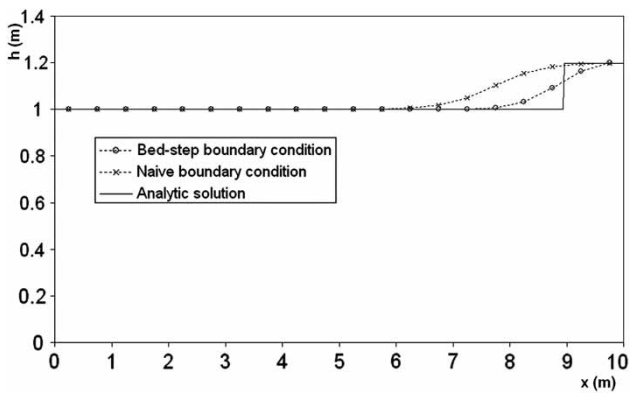

Figure 8 | Subcritical flow chocked at the weir: comparison between the analytical solution and the numerical experiments.

solution, but the strength of the bore and its position are captured correctly by the procedure proposed. In contrast, the results supplied by the naive boundary conditions show that the position of the bore is missed due to the underestimation of the discharge at the beginning of the transient. Results might improve by refining the numerical grid. This example shows that major differences can be found between the solutions obtained with the proposed procedure and the naive boundary conditions also when a subcritical flow approaches the weir. In particular, the complete procedure supplies better results on coarse grids because it can take into account the unbalancing between the boundary condition and the flow upstream of the weir.

CONCLUSIONS

In this paper, it has been shown that the classical weir equation can be regarded as a stationary solution of the Riemann problem for the bottom step shallow-water equations, obtained assuming the energy conservation at the bed step and the dry bed state over the step top. Recalling that this Riemann problem may exhibit multiple solutions for the given initial conditions, for the first time the experimental evidence from the literature has been used to define selection criteria able to extract only the physically congruent solution. Finally, the analytical solution of this special Riemann problem has been exploited in order to implement the broad-crested weir boundary conditions in a finite volume scheme for the solution of the shallow-water equations.

The methodology proposed, which generalizes the non-submerged broad-crested weir formula to transient flow conditions, has been verified using the results of a dam-break laboratory experiment, confirming its ability to reproduce the expected flow behaviour during transients. In order to highlight the merits of the procedure, an exhaustive evaluation has been accomplished comparing its results with those supplied by a naive boundary condition based on the direct use of the weir formula. When the solution is characterized by subcritical flow conditions upstream of the weir, the complete procedure and the naive boundary condition converge to the same solution during a grid refinement process, but the complete procedure supplies more satisfactory results on coarse grids. Moreover, the procedure based on the analytic solution of the weir Riemann problem is able to tackle the case of a supercritical flow that remains supercritical when passing over the broad-crested weir, while the naive boundary conditions cannot discriminate this condition.

In conclusion, the procedure based on the solution of a Riemann problem has a wider application than those based on the direct use of the weir formula, because it incorporates more physical situations, and its results are less sensitive to the grid density. Despite a nontrivial mathematical background, the presented methodology is recommended because it is easy to implement, its computational burden is negligible, and its application is not inhibited by a complicated and scarcely robust numerical machinery.

ACKNOWLEDGEMENTS

The authors want to thank the three anonymous reviewers and the associate editor for their constructive comments, which greatly contributed to improve the paper. Moreover, the first writer wishes to acknowledge the project consortium DE TECH (DEsign cfd and TECHnology)-MI01_00260 for its support.

REFERENCES

Alcrudo, F. & Benkhaldoun, F. 2001 Exact solutions to the Riemann problem of the shallow water equations with a bottom step. *Comput. Fluid.* **30**, 643–671.

Audusse, E., Bouchut, F., Bristeau, M.-O., Klein, R. & Perthame, B. 2004 A fast and stable well-balanced scheme with the hydrostatic reconstruction for shallow water flows. *Siam J. Sci. Comput.* **25**, 2050–2065.

Baines, P. G. & Whitehead, J. A. 2003 On multiple states in single-layers flows. *Phys. Fluids* **15**, 298–307.

Burguete, J., Garcìa-Navarro, P., Murillo, J. & Garcìa-Palacìn, I. 2007 Analysis of the friction term in the one-dimensional shallow-water model. *ASCE J. Hydraul. Eng.* **133**, 1048–1063.

Castro, M. J., Pardo Milanès, A. & Parès, C. 2007 Well-balanced numerical schemes based on a generalized hydrostatic reconstruction technique. *Math. Mod. Meth. Appl. Sci.* **17**, 2055–2113.

Catella, M. & Bechi, G. 2006 Conservative scheme for flow numerical modelling of submerged bridges. In: *RiverFlow 2006 – Proceedings of the International Conference on Fluvial Hydraulics* (E. C. T. L. Alves, A. H. Cardoso, J. G. A. B. Leal & R. M. L. Ferreira, eds). Taylor & Francis/Balkema, London, Vol. 1, pp. 747–755.

Cimorelli, L., Cozzolino, L., Della Morte, R. & Pianese, D. 2013 An improved numerical scheme for the approximate solution of the Parabolic Wave model. *J. Hydroinformat.* **15**, 913–925.

Cimorelli, L., Cozzolino, L., Della Morte, R. & Pianese, D. 2014 Analytical solutions of the linearized parabolic wave accounting for downstream boundary condition and uniform lateral inflows. *Adv Water Resour* **63**, 57–76.

Costabile, P. & Macchione, F. 2012 Analysis of one-dimensional modelling for flood routing in compound channels. *Water Resour. Manage.* **26**, 1065–1087.

Cozzolino, L., Della Morte, R., Covelli, C., Del Giudice, G. & Pianese, D. 2011 Numerical solution of the discontinuous-bottom Shallow-water Equations with hydrostatic pressure distribution at the step. *Adv. Water Resour.* **34**, 1413–1426.

Cozzolino, L., Della Morte, R., Del Giudice, G., Palumbo, A. & Pianese, D. 2012 A well-balanced spectral volume scheme with the wetting-drying property for the shallow-water equations. *J. Hydroinformat.* **14**, 745–760.

Cozzolino, L., Cimorelli, L., Covelli, C., Della Morte, R. & Pianese, D. 2014a A novel numerical approach for 1D variable density shallow flows over uneven rigid and erodible beds. *ASCE J. Hydraul. Eng.* **140**, 254–268.

Cozzolino, L., Della Morte, R., Cimorelli, L., Covelli, C. & Pianese, D. 2014b A broad-crested weir boundary condition in Finite Volume Shallow-water numerical models. *Procedia Engineering* 70, 353–362.

Dal Maso, G., LeFloch, P. G. & Murat, F. 1995 Definition and weak stability of nonconservative products. *Journal de Mathématiques Pures et Appliquées – IX Sèrie* **74**, 483–548.

Domenighetti, A., Vorogushyn, S., Castellarin, A., Merz, B. & Brath, A. 2013 Probabilistic flood hazard mapping: effects of uncertain boundary conditions. *Hydrol. Earth Syst. Sci.* **17**, 3127–3140.

Einfeldt, B. 1988 On Godunov-type methods for gas-dynamics. *Siam J. Numer. Anal.* **25**, 294–318.

Guerra, G., Herty, M. & Marcellini, F. 2011 Modeling and analysis of pooled stepped chutes. *Netw. Heterog. Media* **6**, 665–679.

Hager, W. H. & Sinniger, R. 1985 Flow characteristics of the hydraulic jump in a stilling basin with an abrupt bottom rise. *J. Hydraul. Res.* **23**, 101–113.

Han, E. & Warnecke, G. 2012 The exact Riemann solutions to Shallow-water equations. Available at: http://www.math.ntnu.no/conservation/2012/012.html (accessed May 20 2013).

Hiver, J.-M. 2000 Adverse-slope and slope (bump). In: *Concerted Action on Dam Break Modelling: Objectives, Project Report, Test Cases, Meeting Proceedings* (S. Soares-Frazão, M. Morris & Y. Zech, eds). Universitè Catholique de Louvain, Civil Engineering Department, Hydraulic Division, Louvain-la-Neuve, Belgium (CD-ROM).

Hu, K., Mingham, C. G. & Causon, D. M. 2000 Numerical simulation of wave overtopping of coastal structures using the non-linear shallow water equations. *Coast. Eng. J.* **41**, 433–465.

Karki, K. S., Chander, S. & Malhotra, R. C. 1972 Supercritical flow over sills at incipient jump conditions. *J. Hydraul. Div. ASCE* **98**, 1753–1764.

Kutija, V. & Murray, M. G. 2007 An object-oriented approach to the modelling of free-surface flows. *J. Hydroinformat.* **9**, 81–94.

LeFloch, P. G. & Thanh, M. D. 2011 A Godunov-type method for the Shallow water equations with discontinuous topography in the resonant regime. *J. Comput. Phys.* **230**, 7631–7660.

Mehrotra, S. C. 1974 "Hysteresis" effect in one- and two-fluid systems. In: *Proceedings of the Fifth Australasian Conference on Hydraulics and Fluid Mechanics* (D. Lindley & A. J. Sutherland, eds). University of Canterbury, Christchurch, pp. 452–461.

Morales-Hernàndez, M., Murillo, J. & Garcìa-Navarro, P. 2013 The formulation of internal boundary conditions in unsteady 2-D Shallow-water flows: application to flood regulation. *Water Resour. Res.* **49**, 471–487.

Mynett, A. E. 1999 Hydroinformatics and its applications at Delft Hydraulics. *J. Hydroinformat.* **1**, 83–102.

Ostapenko, V. V. 2002 Discontinuous solutions of the "Shallow water" Equations for flow over a bottom step. *J. Appl. Mech. Tech. Phys.* **43**, 836–846.

Pappenberger, F., Matgen, P., Beven, K. J., Henry, J.-B., Pfister, L. & de Fraipont, P. 2006 Influence of uncertain boundary conditions and model structure on flood inundation predictions. *Adv. Water Resour.* **29**, 1430–1449.

Rebollo, C. T., Fernàndez Nieto, E. D. & Gòmez Marmòl, M. 2003 A flux-splitting solver for shallow water equations with source terms. *Int. J. Numer. Meth. Fluid.* **42**, 23–55.

Schubert, J. E., Sanders, B. F., Smith, M. J. & Wright, N. G. 2008 Unstructured mesh generation and landcover-based resistance for hydrodynamic modelling of urban flooding. *Adv. Water Resour.* **31**, 1603–1621.

Sobey, R. J. 2001 Evaluation of numerical models of flood and tide propagation in channels. *J. Hydraul. Eng.* **127**, 805–824.

Toro, E. F. 2001 *Shock-capturing Methods for Free-surface Shallow Flows*. J. Wiley and Sons, Chichester, UK.

Vidal, J.-P., Moisan, S., Faure, J.-B. & Dartus, D. 2005 Towards a reasoned 1D river model calibration. *J. Hydroinformat.* **7**, 91–104.

Working Group on Small Hydraulic Structures 1989 Discharge measurement structures. In: *International Institute for Land Reclamation and Improvement* (M. G. Bos, ed.). Wageningen, The Netherlands.

Zhao, D. H., Shen, H. W., Tabios III, G. Q., Lai, J. S. & Tan, W. Y. 1994 Finite-volume two-dimensional unsteady-flow model for river basins. *ASCE J. Hydraul. Eng.* **120**, 863–883.

Zhou, J. G., Causon, D. M., Mingham, C. G. & Ingram, D. M. 2004 Numerical prediction of dam-break flows in general geometries with complex bed topography. *J. Hydraul. Eng.* **130**, 332–340.

First received 26 August 2013; accepted in revised form 3 March 2014. Available online 27 March 2014